

Type of the Paper (Article)

1

# The ionic selectivity of lysenin channels in open and sub-conducting states

Andrew Bogard <sup>1,2</sup>, Pangaea W. Finn <sup>1</sup>, Fulton McKinney <sup>1</sup>, Ilinca M. Flacau <sup>1</sup>, Aviana R. Smith <sup>1</sup>, Rosey Whiting <sup>1,2</sup> and Daniel Fologea <sup>1,2,\*</sup>

4

5

<sup>1</sup> Department of Physics, Boise State University, Boise, ID 83725, USA

6

<sup>2</sup> Biomolecular Sciences Graduate Program, State University, Boise, ID 83725, USA

7

\* Correspondence: danielfologea@boisestate.edu

8

**Abstract:** The electrochemical gradients established across cell membranes are paramount for execution of biological functions. Besides ion channels, other transporters, such as exogenous pore-forming toxins, may present ionic selectivity upon reconstitution in natural and artificial lipid membranes and contribute to the electrochemical gradients. In this context, we utilized electrophysiology approaches to assess the ionic selectivity of the pore-forming toxin lysenin reconstituted in planar bilayer lipid membranes. The membrane voltages were determined from the reversal potentials recorded upon channel exposure to asymmetrical ionic conditions, and the permeability ratios calculated from the fit with the Goldman-Hodgkin-Katz equation. Our work shows that lysenin channels are ion-selective and the determined permeability coefficients are cation and anion-species dependent. We also exploited the unique property of lysenin channels to transition to a stable sub-conducting state upon exposure to calcium ions and assessed their subsequent change in ionic selectivity. The observed loss of selectivity was implemented in an electrical model describing the dependency of reversal potentials on calcium concentration. In conclusion, our work demonstrates that this pore-forming toxin presents ionic selectivity but this is adjusted by the particular conduction state of the channels.

9

10

11

12

13

14

15

16

17

18

19

20

21

22

23

**Citation:** Lastname, F.; Lastname, F.; Lastname, F. Title. *Membranes* **2021**, *11*, x. <https://doi.org/10.3390/xxxxx>

24

25

Academic Editor: Firstname Lastname

26

Received: date

27

Accepted: date

28

Published: date

29

**Publisher's Note:** MDPI stays neutral with regard to jurisdictional claims in published maps and institutional affiliations.

30

31

32

33

34

35

36

37

38

39

40

41

42

43

44



**Copyright:** © 2021 by the authors. Submitted for possible open access publication under the terms and conditions of the Creative Commons Attribution (CC BY) license (<https://creativecommons.org/licenses/by/4.0/>).

nels. Lysenin is an intriguing PFT extracted from the red earthworm *E. fetida*, which inserts very stable channels in membranes containing sphingomyelin [13,17,20-24]. The pore-forming mechanism comprises binding to sphingomyelin and deployment of beta-sheets through the host membrane [25,26]. Lysenin exhibits high transport rate, and is also regulated by voltage and ligands [12-14]. Interestingly, the voltage-gating feature requires anionic lipids in the host membrane, and is suppressed when neutral lipids are used [13]. However, the gating induced by multivalent ions acting as ligands is preserved in both neutral and charged lipid membranes [14]. Previous investigations on lysenin suggest a weak cation selectivity [15,17], as inferred from measuring the membrane voltage achieved upon creating asymmetrical ionic conditions. However, these are single point measurements, and no extensive study of the selectivity in various ionic conditions is available. To fill this gap in our knowledge, we employed electrophysiology measurements and expanded the investigations on the selectivity of lysenin channels inserted into planar lipid membranes by considering multiple ions and concentration conditions. These investigations allowed us to provide quantitative analyses of the cation selectivity and show differences between cationic ion species (i.e.,  $\text{Na}^+$ ,  $\text{K}^+$ ,  $\text{Cs}^+$ , and  $\text{Li}^+$ ). In addition, we also demonstrated that lysenin channels present different permeabilities for anionic species (i.e.,  $\text{Cl}^-$ , and  $\text{I}^-$ ). These features, identified for fully-open lysenin channels, resemble the selectivity of ion channels. However, ion channels such as VDAC [27-30], mechano-sensitive, [31-33], sodium [34], and potassium [35,36] may undergo conformational transitions that lead to intermediate, sub-conducting states. Although the physiological relevance of sub-conductance is poorly understood, adjustments of the ionic permeabilities in such sub-conducting states have been reported [27-29]. For a better understanding of how intermediate conductance states adjust the transport properties of protein pores, we exploited a unique feature of lysenin channels, which is the attainment of stable sub-conducting states in the presence of divalent ions (i.e.,  $\text{Ca}^{2+}$ ) [12,14]. In this line, our experimental work demonstrates that the selectivity of lysenin channels to monovalent ions is significantly diminished when they are in the sub-conducting state, which leads to vanishing membrane voltages. The diminished selectivity was assessed by employing a simple electrical model, which in conjunction with the Langmuir isothermal adsorption model describing the divalent ion – channel interaction [12] provided a good match of the experimental data.

## 2. Materials and Methods

### 2.1 Materials

The bilayer lipid membranes (BLMs) utilized for all the experiments described in this work were composed of asolectin (Sigma-Aldrich, St. Louis, MO, USA), cholesterol (Sigma-Aldrich), and sphingomyelin (Avanti Polar Lipids, Alabaster, AL, USA). The lipids in powder form were solubilized in n-decane (TCI America, Portland, OR, USA) and mixed at a 10:4:4 molar ratio for a final concentration of 50 mg asolectin/mL mixture.  $\text{NaCl}$ ,  $\text{KCl}$ ,  $\text{CsCl}$ ,  $\text{LiCl}$ ,  $\text{KI}$ , and  $\text{CaCl}_2$  (ThermoFisher Scientific, Waltham, MA, USA) were dissolved in deionized water and buffered with 20 mM Hepes (ThermoFisher Scientific) for a final pH of 7.2. The utilized solutions were either starting support electrolyte (50 mM salt concentration) or high-concentration stock solutions for ionic additions (2-3 M final concentration).

Lysenin was produced and purified in our Biomolecular Research Center core facility [37] through established protocols [37-40]. Briefly, lysenin cDNA for the full-length protein (accession number D85846) was synthesized and subcloned in pMAL-c5x (GenScript, Piscataway, NJ, USA). This construct generates a maltose binding protein-linked lysenin with a Factor Xa cleavage site between them. Following transformation of the plasmid into *Escherichia coli* BL21 competent cells and purification [37-40], the full-length protein was thoroughly tested for activity and transport properties: channel insertion and voltage regulation [13,17], ligand-induced gating [12,14], and at-

ainment of sub-conducting states in the presence of  $\text{Ca}^{2+}$  ions [12,14]. A stock solution of lysenin dissolved in Phosphate Buffered Saline (PBS1x, pH = 7.2, Sigma-Aldrich) at 1  $\mu\text{g}/\text{mL}$  concentration was utilized for channel reconstitution in artificial membranes. All other common chemicals were purchased from various producers and distributors.

## 2.2 Methods

### 2.2.1 BLM production, characterization, and channel insertion

To investigate the selectivity of lysenin channels we utilized a typical planar BLM setup detailed in prior work [12]. The membrane was formed by the painting method in a small hole (~100  $\mu\text{m}$  diameter) produced in a thin PTFE film (125  $\mu\text{m}$  thickness) by an electric spark. The two ~1mL reservoirs were filled with support electrolyte (50 mM salt, if not otherwise indicated). The electrical connections with the Axopatch 200B amplifier (Molecular Devices, San Jose, CA, USA) were made via Ag/AgCl electrodes connected to the electrolyte solutions through salt bridges made with 2% TopVision Low Melting Point Agarose (ThermoFisher Scientific) and 1M NaCl to minimize the junction potential. The electrodes were wired to the headstage of the electrophysiology amplifier. The signal was digitized with the Digitizer 1440A (Molecular Devices) and recorded on a computer for further analyses. All the experiments were performed at room temperature ( $22.5 \pm 0.5^\circ\text{C}$ ).

The bilayer formation and its integrity were monitored by employing membrane capacitance and conductance measurements. After a stable and intact, non-conducting membrane was formed, channel insertion was initiated by addition of small amounts of lysenin (~0.3 nM final concentration) to the grounded reservoir. Channel insertion was observed as a step-wise variation of the ionic currents recorded at -80 mV bias potential (to avoid the voltage-induced gating) and under solution stirring with a low noise magnetic stirrer (Warner Instruments, Hamden, CT, USA).

### 2.2.3 Voltage measurements

Insertion completion was indicated by stable ionic currents, achieved in approximately one hour after lysenin addition. The amplitude of the macroscopic ionic currents and the unitary conductance of single channels were used to estimate the number of inserted channels, which varied from several hundred to a few thousand for each membrane we used. After stabilization, we determined the membrane voltages originating from the chemical gradients produced by addition of small and known amounts of concentrated ionic solutions to the grounded reservoir. The experimental data were recorded with pClamp 10.6.2.2 (Molecular Devices), plotted with Clampfit 10.6.2.2 (Molecular Devices), and the membrane voltages  $V_m$  determined as the x-intercept of the IV plots (the reversal potentials) recorded for each of the asymmetrical ionic conditions (including symmetrical ionic conditions controls) [7,15,17,18,30]. For each IV plot we set a voltage range of 20 mV and lower and upper limits such that the plots crossed the x axis. A single voltage sweep was set for 20 s, and the sampling rate was set to 10 samples/s (hence a 0.1 mV resolution). As detailed in Figure 1 as an example for NaCl, for each of the concentration ratio ( $c_r$ ) conditions ( $c_r = 1, 2.35$ , and  $5.12$ , respectively) we recorded three sweeps within the same experiment; the excellent overlapping of the sweeps for identical ionic conditions indicates attaining a steady state. The linear fit of the experimental data in Clampfit provided the y-intercepts and slopes, which were next used to determine the x-intercepts (membrane voltages).

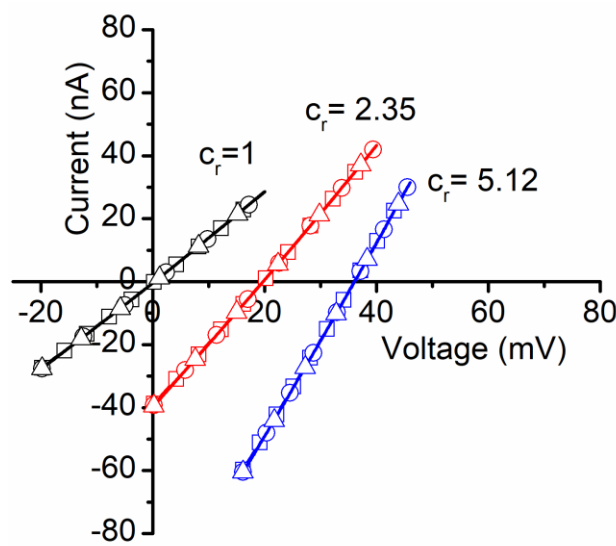


**Figure 1.** Experimental determination of membrane voltages for lysenin channels reconstituted into planar BLMs. Addition of NaCl to the grounded reservoirs leads to a right shift of the IV plots, indicative of membrane voltage occurrence. An individual experiment employed three IV sweeps for each NaCl concentration ratio  $c_r$ , and their average was used to calculate the membrane voltage as the x-intercept. All the points in the plots are experimental; the symbols have been added as visual aids to discriminate between sweeps recorded in identical experimental conditions.

The averaged values of the membrane voltage were determined by using a custom-made analysis program in R, which also calculated the concentration ratios for each of the experimental conditions by accounting for added ions. The averaged membrane voltages and concentration ratios were plotted and fitted (Origin 8.5.1, OriginLab Corporation, Northampton, MA) with the Goldman-Hodgkin-Katz (GHK) equation [7,15-18,30], adjusted for one cation ( $C^+$ ) and one anion ( $A^-$ ) monovalent ion species:

$$Vm = -\frac{RT}{F} \ln \left( \frac{P_{C^+}[C^+]_h + P_{A^-}[A^-]_g}{P_{C^+}[C^+]_g + P_{A^-}[A^-]_h} \right) \quad \text{Eq. 1}$$

where  $R$  is the universal gas constant ( $R=8.31 \text{ J mol}^{-1} \text{ K}^{-1}$ ),  $T$  is the absolute temperature,  $F$  is the Faraday number ( $F = 96,485.35 \text{ C mol}^{-1}$ ),  $P$  denotes the permeabilities of the ionic species, and the square brackets indicates their concentrations in the ground (g) and headstage (h) reservoirs, respectively.

The GHK fit provided the permeability ratio of cations to anions (i.e.,  $P_{C^+}/P_{A^-}$ ) under the assumption that ionic diffusion does not change the ionic concentrations achieved by salt addition, i.e. the concentrations of cations and anions in the same reservoir are equal after electrochemical equilibrium is achieved. This assumption is fully justified by the very small number of ions (relative to the bulk number) needed to diffuse for establishing the membrane voltages. The experiments for determining the membrane voltages and estimating the permeability ratios were independently replicated three times, and the statistical analyses performed in Origin 8.5.1 provided the average values and standard deviations of the permeability ratios. No significant differences in membrane voltages were determined from experiments comprising identical solution conditions but different numbers of inserted channels.

#### 2.2.4 Investigations on sub-conducting channels

To investigate the selectivity of lysenin channels in sub-conducting conditions we utilized buffered KCl (50 mM) solutions as starting support electrolyte. The first set of experiments comprised sub-conductance achievement by addition of  $\text{CaCl}_2$  to both res-

ervoirs (36 mM final concentration), followed by measurements of the membrane voltage upon successive KCl additions to the grounded reservoir. The next set of experiments comprised achieving a membrane voltage by establishing chemical gradients with KCl addition to the grounded reservoir, followed by monitoring the changes in the membrane voltage upon additions of CaCl<sub>2</sub> to both reservoirs. The membrane voltage was determined from the IV plots by following the same procedure described above for monovalent ions. The influence of the Ca<sup>2+</sup> ions on permeability was assessed by employing an electrical model of the membrane and equations detailed in the corresponding results and discussion section.

### 3. Results

#### 3.1 Lysenin channels in open state are cation-selective

The selectivity of lysenin channels for monovalent ions was first investigated for chlorides by additions of small volumes (ranging from 10 to 50  $\mu$ L) of buffered 3M stock solutions to the grounded reservoir. The starting solutions in both reservoirs were buffered 50 mM electrolyte solutions of the same chemical species as stocks, with the exception of experiments that comprised mixtures of chlorides and iodides (detailed in the results section). The control IV plots were run to ensure the absence of any offset transmembrane voltage in symmetrical ionic conditions, after which the membrane voltages were determined for each particular chemical gradient. The results depicted in Figure 2 show typical recordings (i.e., average values obtained from three sweeps within the same experimental setup) and the fit with the GHK equations for NaCl, KCl, CsCl, and LiCl. Subsequent addition of chlorides to the grounded reservoir led to the development of transmembrane voltages with amplitude that increased monotonically with the concentration ratios (Figure 2) for each of the ionic species, which is a direct consequence of ionic selectivity. The P<sub>C+</sub>/P<sub>A</sub>-values determined from three independent experiments for the different ionic compositions are  $22.4 \pm 1.3$  for NaCl,  $7.5 \pm 0.5$  for KCl,  $12.3 \pm 0.5$  for CsCl, and  $12.9 \pm 0.9$  for LiCl. All these values clearly indicate that lysenin channels are slightly selective for cations, as suggested in prior work from single-point measurements [15,17]. Since we have no reason to assume that the permeability of Cl<sup>-</sup> is different when the ions originated in the dissociation of different salts, the different permeability ratio values also indicate that the selectivity of lysenin channels also manifests between cationic species. For example, our experimental results suggest that the permeability for Na<sup>+</sup> is ~3 times larger than the one for K<sup>+</sup>, while Cs<sup>+</sup> and Li<sup>+</sup> have similar permeabilities. Such features are essential for many ion channels; however, their capabilities with regard to discriminating between similar ionic species may attain significantly larger values compared to lysenin channels.

177  
178  
179  
180  
181  
182  
183  
184  
185  
186  
187  
188  
189  
190  
191  
192  
193  
194  
195  
196  
197  
198  
199  
200  
201  
202  
203  
204  
205  
206  
207  
208  
209  
210  
211  
212

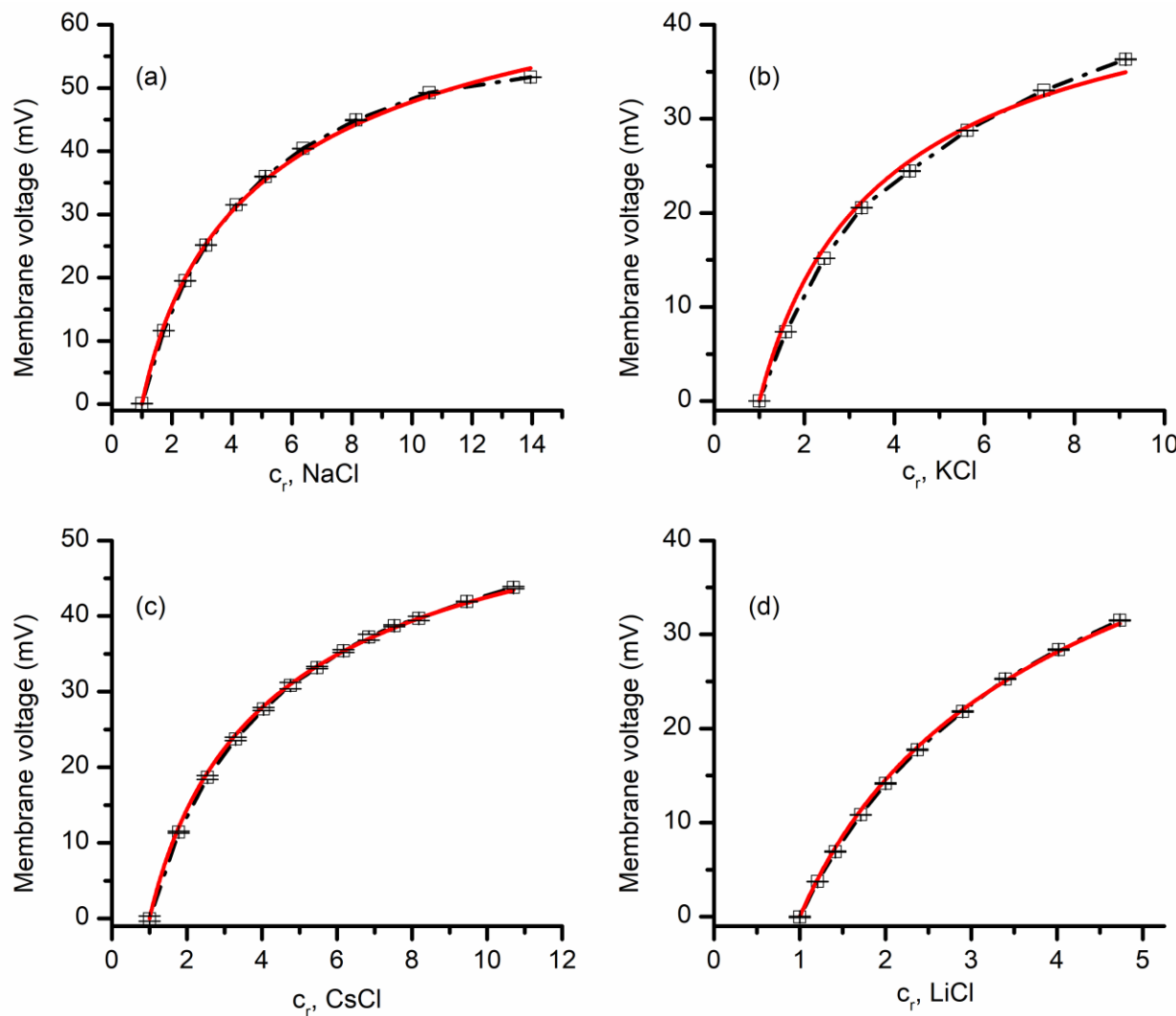


**Figure 2.** Lysenin has selectivity for monovalent cations. The membrane voltage as a function of concentration ratio  $c_r$ , measured for NaCl (a), KCl (b), CsCl (c), and LiCl (d). Each experimental point in the plot (symbols) shows the average value  $\pm$  SD ( $n=3$ ) from three sweeps recorded in single experiments. The full lines are the fit with the GHK equation (single experiments), which was used to determine the permeability ratio of cations over anions from the membrane voltage and concentration ratio  $c_r$  values for each of the indicated ionic species.

### 3.2 Lysenin channels in open state present different permeability for anions

The above experiments provided information with regards to lysenin channels' selectivity for cations versus anions, together with an indication that lysenin also discriminates between similar cation species. Next, we asked whether lysenin channels present different selectivity for similar anion species. To answer this question, we ran experiments employing KI for the 50 mM support electrolyte and a 3 M KI stock solution for creating chemical gradients. The plot of the transmembrane voltage versus concentration ratio depicted in Figure 3 shows that a concentration ratio of ~5 led to a transmembrane voltage of ~32 mV. This value is slightly larger than what was obtained for a similar KCl ratio (see Figure 2), indicative of different permeabilities of I<sup>-</sup> and Cl<sup>-</sup> ions. The permeability ratio  $P_{C+}/P_A$  determined from the GHK equation for KI (i.e.,  $27.3 \pm 0.7$ ) was larger than what we obtained for the KCl case (~7.5); this result suggests that the lysenin's permeability for I<sup>-</sup> is a few times smaller than for Cl<sup>-</sup>. Since the two permeabilities are different, we predicted that the membrane voltages established across a membrane containing lysenin channels would be different from addition of KI over KCl support solu-

213  
214  
215  
216  
217  
218  
219  
220  
221  
222  
223  
224  
225  
226  
227  
228  
229  
230  
231  
232  
233  
234

tions, or KCl over KI. This prediction was confirmed experimentally (Figure 3). Addition of KCl over KI support electrolyte produced a membrane voltage significantly smaller than what was measured for the same concentration ratios when KI was added over KCl. Moreover, addition of KCl over KI resembled the KCl-only behavior (shown in Figure 2), while KI addition over KCl was rather similar to the KI-only measurements (Figure 3a). 235  
236  
237  
238  
239

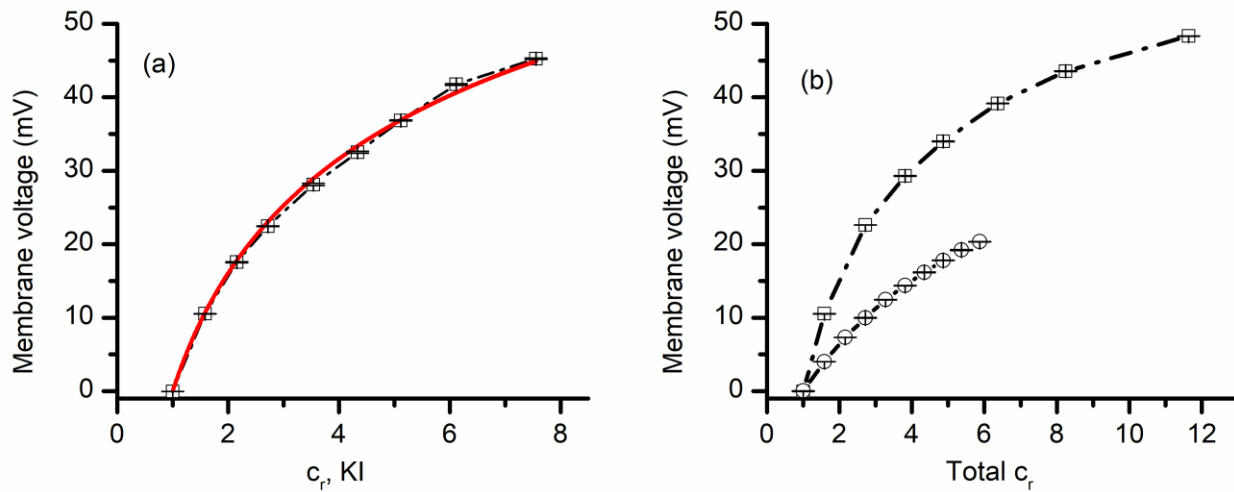


**Figure 3.** Lysenin channels present different permeability for anions. The membrane voltage as a function of concentration ratio measured for KI addition to a KI support electrolyte solution (a). The full line is the fit with the GHK equation, which was used to determine the permeability ratio of  $\text{K}^+$  over  $\text{I}^-$ . Panel (b) shows the measured membrane voltage as a function of total salt concentration ratio when KI was added over 50 mM KCl (open circles), or KCl was added over 50 mM KI (open squares) to the grounded reservoir. The dashed line is used as a visual aid. For each panel, the experimental points in the plot (symbols) show the average value  $\pm \text{SD}$  ( $n=3$ ) from three sweeps recorded in individual experiments. 240  
241  
242  
243  
244  
245  
246  
247  
248

### 3.3 Investigations on the selectivity of lysenin channels in sub-conducting states

Our next investigations focused on less explored aspects of gated channels, which are potential hidden changes of their biophysical properties that occur when the conformational changes lead to transitions to sub-conducting states. Several channels are known to undergo sub-conducting states [29,31], i.e. an intermediate state between open and closed, characterized by a non-zero, intermediate conductance. The physiological relevance of such sub-conducting states is still unclear [28], and deep investigations of such aspects are hindered not only by the limited channel species that present such states, but also by a certain inability to control these generally unstable states. Lysenin is a notable exception, and prior experiments demonstrate that lysenin channels may be forced to adopt a stable sub-conducting state upon exposure to divalent organic and inorganic divalent cations [12]. For example,  $\text{Ca}^{2+}$  or  $\text{Mg}^{2+}$  at concentrations over 20 mM force the lysenin channels to adopt a stable half-closed state, for which the conductance is ~20% of the conductance of a fully open channel [12]. Therefore, we exploited this remarkable property of lysenin channels to investigate their selectivity in sub-conducting states and compare it with the open state. To achieve this objective, we first tested the development of a transmembrane voltage by imposing non-symmetrical ionic concentrations of KCl upon a membrane containing sub-conducting lysenin channels. In this respect, we used a typical experimental approach for inserting fully open lysenin channels in a membrane bathed by 50 mM KCl. After stabilization, we added 36 mM  $\text{CaCl}_2$  to both reservoirs to force the channels to transition to a sub-conducting state. Although prior work suggests that  $\text{Ca}^{2+}$  ions permeate the lysenin channels in both open and sub-conducting states [12], we added  $\text{CaCl}_2$  to both sides to avoid asymmetrical divalent ion concentrations potentially leading to supplementary membrane voltages; the absence of such a voltage was 249  
250  
251  
252  
253  
254  
255  
256  
257  
258  
259  
260  
261  
262  
263  
264  
265  
266  
267  
268  
269  
270  
271  
272

verified by running an IV plot from -10 mV to 10 mV, which showed the absence of any ionic current at 0 mV (Figure 4). Next, we exposed the grounded side of the membrane to increased concentrations of KCl by adding to it small amounts of the 3M KCl solution. To our surprise, none of the additions revealed a transmembrane voltage larger than a few mV (Figure 4) even for concentrations for which we otherwise measured tens of mV in the absence of  $\text{Ca}^{2+}$  (as shown in Figure 2).

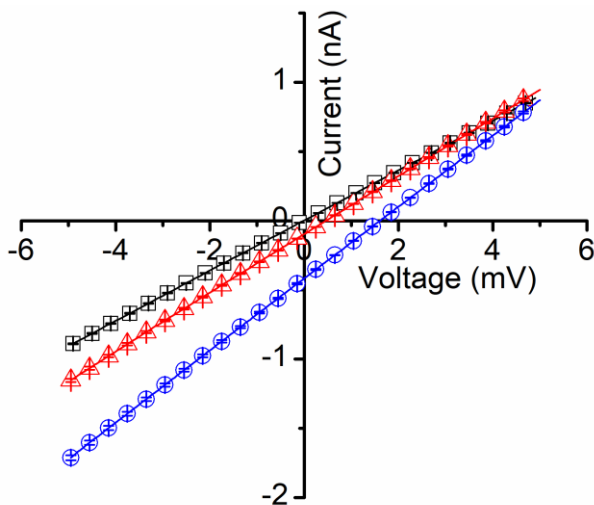


**Figure 4.** Lysenin's selectivity is diminished in sub-conducting states. After exposure of lysenin channels to 36 mM  $\text{Ca}^{2+}$  ions (for inducing stable sub-conducting states), symmetrical KCl concentration conditions indicated the absence of any membrane voltage (open squares). KCl addition to the ground side (concentration ratio of 3 (open triangles), and 13 (open circles), respectively) led to the development of negligible membrane voltages, in the mV range. All the data in the plots are experimental; the symbols have been added as a visual aid, and they represent average values  $\pm$  SD from three IV sweeps recorded in the same experiments.

A reasonable assumption for this unexpected behavior would be the loss of selectivity for channels in the sub-conducting state. We excluded the hypothesis that no ions may move through sub-conducting channels since the ionic conductance in the sub-conducting state is still very large. To reasonably explain the diminished membrane voltage observed experimentally, we modeled the membrane containing lysenin channels in either state by a combination of a voltage source (fully open channels), a serial resistance ( $R_1$ , the resistance of the fully open channels), and another resistance ( $R_2$ ) parallel to the entire assembly and representing all the sub-conducting channels (Figure 5). For slow-varying voltage measurements the capacitance of the membrane may be neglected. Also, although the channels may present a very weak selectivity in the sub-conducting state, we opted to exclude a second voltage source for these channels since the results presented in Figure 4 show only a negligible voltage for sub-conducting channels exposed to asymmetrical KCl conditions. This low resting voltage also suggests that  $\text{CaCl}_2$  addition, although changes the  $\text{Cl}^-$  concentrations on both sides of the membrane, has at most a small contribution to the membrane voltage. Therefore, the monovalent ions may be considered the major contributors to the membrane voltage for these experimental conditions, which simplifies the electrical model of the membrane.



**Figure 5.** The electrical model for a membrane containing lysenin channels in both open and sub-conducting states. The model includes a voltage source  $V$ , open channels of total resistance  $R_1$ , and sub-conducting channels of total resistance  $R_2$ . The resulting membrane voltage  $V_m$  may be estimated from the electrical parameters of the equivalent circuit.

The membrane voltage for the model shown in Figure 5 may be calculated from Ohm's law:

$$V_m = V \frac{R_2}{R_1 + R_2} \quad \text{Eq. 2}$$

The other premises of the proposed model are as follows: i) the membrane contains  $N$  channels, from which  $n_1$  are in the open state and  $n_2$  in the sub-conducting state ( $N = n_1 + n_2$ ); ii) for given ionic conditions the resistance of an individual open channel is  $r_1$ , and the resistance of an individual sub-conducting channel is  $r_2$ ; and iii) the ratio between the individual resistances of sub-conducting and conducting channels in otherwise identical solution conditions is  $r_1/r_2 = f = 0.2$  [12]. With these assumptions, the membrane voltage becomes:

$$V_m = \frac{V}{\left( \frac{fn_2}{N - n_2} \right) + 1} \quad \text{Eq. 3}$$

Assessing the evolution of the membrane voltage when variable populations of fully conducting and sub-conducting channels coexist in the membrane requires estimating  $n_2$ . This was previously performed by considering the interactions between  $\text{Ca}^{2+}$  ions and lysenin channels a Langmuir isothermal adsorption process [12], for which:

$$n_2 = \frac{K[\text{Ca}^{2+}]N}{1 + K[\text{Ca}^{2+}]} \quad \text{Eq. 4}$$

where  $K$  is the Langmuir constant,  $[\text{Ca}^{2+}]$  is  $\text{Ca}^{2+}$  concentration in the bulk solution, and  $N$  is the total number of lysenin channels inserted into the membrane.

The combination of the last two equations leads to a simplified formula for the membrane voltage:

$$V_m = \frac{V}{fK[\text{Ca}^{2+}] + 1} \quad \text{Eq. 5}$$

The last equation predicts that the membrane voltage established from chemical gradients must monotonically decrease with increasing  $\text{Ca}^{2+}$  concentration. To verify this hypothesis, we measured the variation of the membrane voltage created by KCl gradients upon successive  $\text{Ca}^{2+}$  addition. We utilized buffered KCl (50 mM) support electrolyte and created a membrane voltage of ~22.4 mV by adding KCl to the grounded reservoir (for a concentration ratio of 4.1). Addition of  $\text{Ca}^{2+}$  up to 25 mM to both reservoirs decreased the membrane voltage in a concentration-dependent manner, as predicted by Eq. 5 (Figure 6). The plot was fit with Eq. 5, in which we utilized an  $f$  value of 0.2, as previ-

ously determined from conductance measurements [12]. The fit provided a  $K$  value of  $0.32 \pm 0.07$  mM ( $n = 2$ ). This Langmuir constant is several times larger than what was determined from macroscopic conductance measurements (i.e.,  $K = 0.05$  mM [12]). However, those experiments were performed by utilizing 150 mM salt for the support electrolyte, and our experiments employed 50 mM. Since the primary interaction between divalent metal cations and lysenin channels is presumably electrostatic [12], one may easily anticipate that a lower ionic strength of the solution environment augments the electrostatic interactions by reducing ionic screening; as our experimental determinations indicate, this clearly leads to an increased adsorption constant .

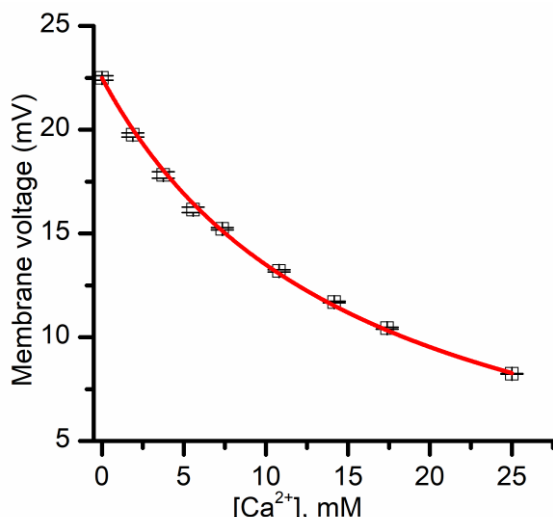


**Figure 6.** Influence of  $\text{Ca}^{2+}$  ions on the transmembrane voltage resulting from asymmetrical KCl salt conditions. The membrane voltage (averaged from three sweeps) is diminished upon  $\text{Ca}^{2+}$  addition to both sides of the membrane, suggesting that lysenin channels in sub-conducting states have reduced selectivity. The continuous line is the fit with Eq. 5.

Ionic selectivity is a salient feature of ion channels, largely utilized for establishing fundamental physiological processes in all living systems. Our work demonstrates that lysenin channels also present ionic selectivity, and that the permeability is different for monovalent anions and cations. Although the permeability ratios are much smaller than what is typically encountered for many ion channels, the selectivity function may lead to the development of large resting potentials, comparable to the ones measured for cells. Consequently, this may be further exploited to modulate the membrane voltage of natural membrane systems. Lysenin reconstitution into artificial membrane systems (i.e., liposomes) may provide the means to create electrochemical gradients to be utilized for energy production and control of metabolic processes in synthetic cell-like systems. The ability of lysenin to attain stable sub-conducting states allowed us to investigate its selectivity to monovalent ions, which was significantly diminished. To explain the loss of this function, one may consider it an effect originating in the binding of  $\text{Ca}^{2+}$  ions to the channel, which will change the electrostatic properties and the energy landscape. However, this may require a direct binding to the selectivity filter in order to annihilate its function. Another hypothesis, which we consider more attractive, is that the channel's conformational changes during the transition from the open to sub-conducting state [12] leads to a displacement of the selectivity filter, hence hindering its function.

The selectivity function presented by lysenin, together with the high transport rate and exquisite regulation by voltage and ligands, closely resembles the salient features of ion channels. It is not clear why a pore-forming toxin meant to kill the target cells is endowed with such remarkable functionalities, which are rather descriptive of ion channels. In this respect, the hypothesis that lysenin is part of a defense system is not fully

supported by its unusual characteristics. Future extended work is needed to better understand the ionic permeability of lysenin channels in open and sub-conducting states, identify conformational changes induced by divalent ions, elucidate their physiological role, and develop applications emerging from its unique biophysical properties.	378 379 380 381 382
<b>Author Contributions:</b> Conceptualization, A.B. and D.F.; methodology, A.B. and D.F.; software, I.M.F., P.W.F, and D.F.; validation, A.B, R.W. and D.F.; investigation, A.B., P.W.F, F.M., I.M.F., A.R.S., R.W. and D.F.; protein production and characterization, R.W.; resources, D.F.; supervision and project administration, A.B. and D.F. All authors contributed to original draft preparation, review, editing, and have read and agreed to the final version of the manuscript.	383 384 385 386 387
<b>Funding:</b> This research was funded by the National Science Foundation (grant number 1554166) and National Institute of Health (grant numbers P20GM103408 and P20GM109095).	388 389
<b>Acknowledgments:</b> I.M.F. is a student at Leland High School, San Jose, CA, USA, who contributed to experimental and theoretical approaches of this work during a summer internship at Boise State University. I.M.F. created the custom R program for analysis, which can be found here: <a href="https://github.com/iiflacauf/Electrophysiological-Analysis/commit/2b64981b50236e51e109c6755bc3dc1469e84a48">https://github.com/iiflacauf/Electrophysiological-Analysis/commit/2b64981b50236e51e109c6755bc3dc1469e84a48</a>	390 391 392 393 394
<b>Conflicts of Interest:</b> The authors declare no conflict of interest. The funders had no role in the design of the study; in the collection, analyses, or interpretation of data; in the writing of the manuscript, or in the decision to publish the results.	395 396 397
<b>References</b>	398 399
1. Hille, B. <i>Ion channels of excitable membranes</i> , 3rd ed.; Sinauer Associates, Inc., Sunderland, MA, USA, 2001.	400 401
2. Bezanilla, F.; Ion Channels: From Conductance to Structure. <i>Neuron</i> <b>2008</b> , <i>60</i> , 456–468, DOI:10.1016/j.neuron.2008.10.035.	402
3. Carvalho-de-Souza, J.L.; Saponaro, A.; Bassetto, C.A.Z.; Rauh, O.; Schroeder, I.; Franciolini, F.; Catacuzzeno, L.; Bezanilla, F.; Thiel, G.; Moroni, A. Experimental challenges in ion channel research: uncovering basic principles of permeation and gating in potassium channels. <i>Adv. Phys.- X</i> <b>2022</b> , <i>7</i> , 1978317, DOI:10.1080/23746149.2021.1978317.	403 404 405
4. de Lera Ruiz, M.; Kraus, R.L. Voltage-Gated Sodium Channels: Structure, Function, Pharmacology, and Clinical Indications. <i>J. Med. Chem.</i> <b>2015</b> , <i>58</i> , 7093–7118, DOI:10.1021/jm501981g.	406 407
5. Dudev, T.; Lim, C. Ion Selectivity Strategies of Sodium Channel Selectivity Filters. <i>Acc. Chem. Res.</i> <b>2014</b> , <i>47</i> , 3580–3587, DOI:10.1021/ar5002878.	408 409
6. Roux, B. Ion channels and ion selectivity. <i>Essays Biochem.</i> <b>2017</b> , <i>61</i> , 201–209, DOI:10.1042/EBC20160074.	410
7. Cymes, G.D.; Grosman, C. Identifying the elusive link between amino acid sequence and charge selectivity in pentameric ligand-gated ion channels. <i>Proc. Nat. Acad. Sci. U.S.A.</i> <b>2016</b> , <i>113</i> , E7106, DOI:10.1073/pnas.1608519113.	411 412
8. Westhoff, M.; Eldstrom, J.; Murray, C.I.; Thompson, E.; Fedida, D. $I_K$ ion-channel pore conductance can result from individual voltage sensor movements. <i>Proc. Nat. Acad. Sci. U.S.A.</i> <b>2019</b> , <i>116</i> , 7879–7888, DOI:10.1073/pnas.1811623116.	413 414
9. Abdul Kadir, L.; Stacey, M.; Barrett-Jolley, R. Emerging Roles of the Membrane Potential: Action Beyond the Action Potential. <i>Front. Physiol.</i> <b>2018</b> , <i>9</i> , DOI:10.3389/fphys.2018.01661.	415 416
10. Peraro, M.D.; van der Goot, F.G. Pore-forming toxins: ancient, but never really out of fashion. <i>Nat. Rev. Microbiol.</i> <b>2016</b> , <i>14</i> , 77–92, DOI:10.1038/nrmicro.2015.3.	417 418
11. Bainbridge, G.; Gokce, I.; Lakey, J.H. Voltage gating is a fundamental feature of porin and toxin $\beta$ -barrel membrane channels. <i>FEBS Lett.</i> <b>1998</b> , <i>431</i> , 305–308, DOI:10.1016/S0014-5793(98)00761-3.	419 420
12. Fologea, D.; Krueger, E.; Al Faori, R.; Lee, R.; Mazur, Y.I.; Henry, R.; Arnold, M.; Salamo, G.J. Multivalent ions control the transport through lysenin channels. <i>Biophys. Chem.</i> <b>2010</b> , <i>152</i> , 40–45, DOI:10.1016/j.bpc.2010.07.004.	421 422
13. Ide, T.; Aoki, T.; Takeuchi, Y.; Yanagida, T. Lysenin forms a voltage-dependent channel in artificial lipid bilayer membranes. <i>Biochem. Biophys. Res. Commun.</i> <b>2006</b> , <i>346</i> , 288–292, DOI:10.1016/j.bbrc.2006.05.115.	423 424
14. Bogard, A.; Abatchev, G.; Hutchinson, Z.; Ward, J.; Finn, P.W.; McKinney, F.; Fologea, D. Lysenin Channels as Sensors for Ions and Molecules. <i>Sensors</i> <b>2020</b> , <i>20</i> , 6099, DOI:10.3390/s20216099.	425 426
15. Aoki, T.; Hirano, M.; Takeuchi, Y.; Kobayashi, T.; Yanagida, T.; Ide, T. Single channel properties of lysenin measured in artificial lipid bilayers and their applications to biomolecule detection. <i>Proc. Jpn. Acad., Ser. B</i> <b>2010</b> , <i>86</i> , 920–925, DOI:10.2183/pjab.86.920.	427 428 429

16. Gu, L.-Q.; Dalla Serra, M.; Vincent, J.B.; Vigh, G.; Cheley, S.; Braha, O.; Bayley, H. Reversal of charge selectivity in trans-membrane protein pores by using noncovalent molecular adapters. *Proc. Nat. Acad. Sci. U.S.A.* **2000**, *97*, 3959–3964, DOI:10.1073/pnas.97.8.3959. 430  
431  
432

17. Kwiatkowska, K.; Hordejuk, R.; Szymczyk, P.; Kulma, M.; Abdel-Shakor, A.-B.; Plucienniczak, A.; Dolowy, K.; Szewczyk, A.; Sobota, A. Lysenin-His, a sphingomyelin-recognizing toxin, requires tryptophan 20 for cation-selective channel assembly but not for membrane binding. *Mol. Membr. Biol.* **2007**, *24*, 121–134, DOI:10.1080/09687860600995540. 433  
434  
435

18. Nestorovich, E.M.; Karginov, V.A.; Bezrukov, S.M. Polymer partitioning and ion selectivity suggest asymmetrical shape for the membrane pore formed by epsilon toxin. *Biophys. J.* **2010**, *99*, 782–789, DOI:10.1016/j.bpj.2010.05.014. 436  
437

19. Ostolaza, H.; Gonzalez-Bullon, D.; Uribe, K.B.; Martin, C.; Amuategi, J.; Fernandez-Martinez, X. Membrane Permeabilization by Pore-Forming RTX Toxins: What Kind of Lesions Do These Toxins Form? *Toxins* **2019**, *11*, 354, DOI:10.3390/toxins11060354. 438  
439  
440

20. Shogomori, H.; Kobayashi, T. Lysenin: A sphingomyelin specific pore-forming toxin. *Biochim. Biophys. Acta Gen. Subj.* **2008**, *1780*, 612–618, DOI:10.1016/j.bbagen.2007.09.001. 441  
442

21. Yamaji-Hasegawa, A.; Makino, A.; Baba, T.; Senoh, Y.; Kimura-Suda, H.; Sato, S.B.; Terada, N.; Ohno, S.; Kiyokawa, E.; Umeda, M.; Kobayashi, T. Oligomerization and pore formation of a sphingomyelin-specific toxin, lysenin. *J. Biol. Chem.* **2003**, *278*, 22762–22770, DOI:10.1074/jbc.M213209200. 443  
444  
445

22. Yilmaz, N.; Yamada, T.; Greimel, P.; Uchihashi, T.; Ando, T.; Kobayashi, T. Real-Time Visualization of Assembling of a Sphingomyelin-Specific Toxin on Planar Lipid Membranes. *Biophys. J.* **2013**, *105*, 1397–1405, DOI:10.1016/j.bpj.2013.07.052. 446  
447

23. Shakor, A.-B.A.; Czurylo, E.A.; Sobota, A. Lysenin, a unique sphingomyelin-binding protein. *FEBS Lett.* **2003**, *542*, 1–6, DOI:10.1016/S0014-5793(03)00330-2. 448  
449

24. Bruhn, H.; Winkelmann, J.; Andersen, C.; Andra, J.; Leippe, M. Dissection of the mechanisms of cytolytic and antibacterial activity of lysenin, a defense protein of the annelid *Eisenia fetida*. *Dev. Comp. Immunol.* **2006**, *30*, 597–606, DOI:10.1016/j.dci.2005.09.002. 450  
451  
452

25. Yilmaz, N.; Kobayashi, T.; Assemblies of pore-forming toxins visualized by atomic force microscopy. *Biochim. Biophys. Acta - Biomembr.* **2016**, *1858*, 500–511, DOI:10.1016/j.bbamem.2015.11.005. 453  
454

26. Yilmaz, N.; Yamaji-Hasegawa, A.; Hullin-Matsuda, F.; Kobayashi, T.; Molecular mechanisms of action of sphingomyelin-specific pore-forming toxin, lysenin. *Semin. Cell Dev. Biol.* **2018**, *73*, 188–198, DOI:10.1016/j.semcd.2017.07.036. 455  
456

27. Najbauer, E.E.; Becker, S.; Giller, K.; Zweckstetter, M.; Lange, A.; Steinem, C.; de Groot, B.L.; Griesinger, C.; Andreas, L.B. Structure, gating and interactions of the voltage-dependent anion channel. *Eur. Biophys. J.* **2021**, *50*, 159–172, DOI:10.1007/s00249-021-01515-7. 457  
458  
459

28. Sander, P.; Gudermann, T.; Schredelseker, J. A Calcium Guard in the Outer Membrane: Is VDAC a Regulated Gatekeeper of Mitochondrial Calcium Uptake? *Int. J. Mol. Sci.* **2021**, *22*, 946, DOI:10.3390/ijms22020946. 460  
461

29. Briones, R.; Weichbrodt, C.; Paltrinieri, L.; Mey, I.; Villinger, S.; Giller, K.; Lange, A.; Zweckstetter, M.; Griesinger, C.; Becker, S.; Steinem, C.; de Groot, B.L. Voltage Dependence of Conformational Dynamics and Subconducting States of VDAC-1. *Biophys. J.* **2016**, *111*, 1223–1234, DOI:10.1016/j.bpj.2016.08.007. 462  
463  
464

30. Gincel, D.; Silberberg, S.D.; Shoshan-Barmatz, V. Modulation of the Voltage-Dependent Anion Channel (VDAC) by Glutamate. *J. Bioenerg. Biomembr.* **2000**, *32*, 571–583, DOI:10.1023/a:1005670527340. 465  
466

31. Cox, C.D.; Nomura, T.; Ziegler, C.S.; Campbell, A.K.; Wann, K.T.; Martinac, B. Selectivity mechanism of the mechanosensitive channel MscS revealed by probing channel subconducting states. *Nat. Commun.* **2013**, *4*, 2137, DOI:10.1038/ncomms3137. 467  
468  
469

32. Flegler, V.J.; Rasmussen, T.; Böttcher, B. More Than Just Closed and Open: Unraveling a Mechanosensor. *Trends Bioche. Sci.* **2021**, *46*, 623–625, DOI:10.1016/j.tibs.2021.04.002. 470  
471

33. Shapovalov, G.; Lester, H.A. Gating transitions in bacterial ion channels measured at 3 microns resolution. *J. Gen. Physiol.* **2004**, *124*, 151–161, DOI:10.1085/jgp.200409087. 472  
473

34. Jo, A.; Hoi, H.; Zhou, H.; Gupta, M.; Montemagno, C.D.; Single-molecule study of full-length NaChBac by planar lipid bilayer recording. *PLOS ONE* **2017**, *12*, e0188861. DOI:10.1371/journal.pone.0188861 474  
475

35. Chapman, M.L.; VanDongen, A.M.J.; K Channel Subconductance Levels Result from Heteromeric Pore Conformations. *J. Gen. Physiol.* **2005**, *126*, 87–103, DOI:10.1085/jgp.200509253. 476  
477

36. Cheng, W.W.L.; Enkvetchakul, D.; Nichols, C.G.; KirBac1.1: It's an Inward Rectifying Potassium Channel. *J. Gen. Physiol.* **2009**, *133*, 295–305, DOI:10.1085/jgp.200810125. 478  
479

37. Warner, L.R.; Mass, O.; Donnelly, L.N.; Grantham, B.R.; Oxford, J.T. Growing and Handling of Bacterial Cultures within a Shared Core Facility for Integrated Structural Biology Program. In *Growing and Handling of Bacterial Cultures*, Mishra, M., Ed.; IntechOpen Limited, London, UK, 2018, DOI:10.5772/intechopen.81932. 480  
481  
482

38. Duong-Ly, K.C.; Gabelli, S.B.; Lorsch, J.R. Affinity Purification of a Recombinant Protein Expressed as a Fusion with the Maltose-Binding Protein (MBP) Tag. In *Methods in Enzymology*, Lorsch, J.R., Ed.; Academic Press, 2015; Vol. 559, pp. 17–26. DOI:10.1016/bs.mie.2014.11.004. 483  
484  
485

39. Jenny, R.J.; Mann, K.G.; Lundblad, R.L. A critical review of the methods for cleavage of fusion proteins with thrombin and factor Xa. *Protein Expr. Purif.* **2003**, *31*, 1-11, DOI:10.1016/S1046-5928(03)00168-2. 486  
487

40. Lebendiker, M.; Danieli, T. Purification of Proteins Fused to Maltose-Binding Protein. In *Protein Chromatography: Methods and Protocols*, Walls, D., Loughran, S.T., Eds.; Humana Press, New York, NY, 2017; pp. 257-273. 488  
489  
DOI:10.1007/978-1-4939-6412-3\_13. 490  
491